

Sound Intensity Scaling for Power-Plant Noise Source Ranking

Paul Zeng, Vince Solferino and Bill Baldwin, Ford Motor Company, Dearborn, Michigan

Power-plant noise source ranking is a sound power contribution analysis of components within 1/3-octave frequency bands at different engine speeds. Such an analysis is required for cascading a given power-plant NVH target to individual components.¹ In NVH roadmap development, this analysis can estimate the NVH benefit of individual NVH actions. Sound intensity scaling is a necessary part of this technique.

Traditionally, sound intensity measurements have been used for power-plant source ranking. These measurements require that an operator be inside the test cell and they are limited to low engine speeds due to safety requirements. For high-speed source ranking, sound intensity is estimated from sound pressure measurements. This method is based on the theoretical model that the sound intensity ratio of any two speeds is equal to the sound pressure ratio squared. By tracking sound pressure change, sound intensity can be estimated from one speed to another. This can be done in two steps: 1) calculate the differences in sound pressure levels (SPLs) from near field measurements at each 1/3-octave band between baseline sound intensity measurements at low speeds; 2) the sound intensity at high speeds can then be calculated by adding those differences to the baseline sound intensity level at corresponding 1/3 octave bands. The method is simple, reliable, and practical.

Several other methods are also available, like spatial transformation of sound fields, structural vibration measurements and laser vibrometer measurements. These methods have limitations that make it impossible or impractical for source ranking applications.

Sound Intensity Scaling Theory

To develop a relationship between sound intensity and sound pressure at different engine speeds, we divide a component into l small elements, as shown in Figure 1. These elements can be treated as point monopole sound sources. Assuming that element x has a source strength $Q_x(t)$, the sound pressure $p_{nx}(r_x, t)$, particle velocity $u_{nx}(r_x, t)$, and sound intensity $I_{nx}(r_x, t)$ at point n with a distance r_x are given by Equations 2, 3, and 4.^{2,3}

$$Q(t)_x = s_x U(t)_x \quad (1)$$

where:

$Q(t)_x$ = element x strength, in³/sec

s_x = area of element x , in²

$U(t)_x$ = average velocity of element x , in/sec

$$p_{nx}(r_x, t) = jk\rho_0 c_0 \frac{s_x U(t)_x}{4\pi r_x} e^{-jkr_x} \quad (2)$$

$$u_{nx}(r_x, t) = (1 + jkr_x) \frac{s_x U(t)_x}{4\pi r_x^2} e^{-jkr_x} \quad (3)$$

$$I_{nx}(r_x, t) = \frac{p_{nx}(r_x, t)^2}{\rho_0 c_0} \left(1 + \frac{1}{jkr_x}\right) \quad (4)$$

where:

$k = 2\pi/\lambda$, wave number, 1/in

ρ_0 = ambient density, lb_m/in³

c_0 = wave speed, in/sec

r_x = distance between element x and point n , inch

$j = \sqrt{-1}$

To calculate the sound intensity due to element i , $U(t)_x$ is chosen as a reference. The average velocity at element i is expressed in terms of the reference velocity multiplied by an amplitude adjustment and a phase adjustment. The sound pressure and sound intensity at point n due to element i can be expressed as:

$$p_{ni}(r_i, t) = jk\rho_0 c_0 \frac{a_i s_x U(t)_x}{4\pi b_i r_x} e^{-jkb_i r_x} e^{-j\theta_i} \quad (5)$$

$$= p_{nx}(r_x, t) \frac{a_i}{b_i} e^{-j2(kb_i r_x + \theta_i - kr_x)}$$

$$I_{ni}(r_i, t) = \frac{p_{ni}(r_i, t)^2}{\rho_0 c_0} \left(1 + \frac{1}{jkr_i}\right) \quad (6)$$

$$= \frac{p_{nx}(r_x, t)^2}{\rho_0 c_0} \left(1 + \frac{1}{jkb_i r_x}\right) \left(\frac{a_i}{b_i}\right)^2 e^{-j2(kb_i r_x + \theta_i - kr_x)}$$

where:

a_i = amplitude adjustment ratio between elements i and x at frequency f

r_i = distance between element i and point n , inches

b_i = distance ratio between r_x and r_i

θ_i = phase difference at measurement point of pressure contributions from elements x and i

The total contributions of sound pressure and intensity at the measurement point of all elements is given by Equations 7 and 8:

$$p_n(t) = p_{nx}(r_x, t) \sum_{i=1}^l \frac{a_i}{b_i} e^{-j(kb_i r_x + \theta_i - kr_x)} \quad (7)$$

$$I_n(t) = \sum_{i=1}^l I_{ni}(r_i, t) = \frac{p_{nx}(r_x, t)^2}{\rho_0 c_0} \quad (8)$$

$$\times \sum_{i=1}^l \left(\frac{1}{jkb_i r_x}\right) \left(\frac{a_i}{b_i}\right)^2 e^{-j2(kb_i r_x + \theta_i - kr_x)}$$

where l is the total number of the elements of the component in Figure 1. The relationship between $p_n(t)$ and $I_n(t)$ can be found by substituting Equation 7 for 8:

$$I_n(t) = \frac{p_n(t)^2}{\rho_0 c_0} \frac{\sum_{i=1}^l \left(1 + \frac{1}{jkb_i r_x}\right) \left(\frac{a_i}{b_i}\right)^2 e^{-j2(kb_i r_x + \theta_i - kr_x)}}{\sum_{i=1}^l \frac{a_i}{b_i} e^{-j(kb_i r_x + \theta_i - kr_x)}} \quad (9)$$

The relationship between two test conditions at t_1 and t_2 is given by Equation 10:

$$\frac{I_n(t_1)}{I_n(t_2)} = \frac{p_n(t_1)^2}{p_n(t_2)^2} \quad (10)$$

$$\frac{\sum_{i=1}^l \left(1 + \frac{1}{jkb_i r_x}\right) \left(\frac{a_i}{b_i}\right)^2 e^{-j2(kb_i r_x + \theta_i - kr_x)}}{\sum_{i=1}^l \frac{a_i}{b_i} e^{-j(kb_i r_x + \theta_i - kr_x)}} \Bigg|_{(t_1)} \times \frac{\sum_{i=1}^l \left(\frac{a_i}{b_i}\right)^2 e^{-j2(kb_i r_x + \theta_i - kr_x)}}{\sum_{i=1}^l \frac{a_i}{b_i} e^{-j(kb_i r_x + \theta_i - kr_x)}} \Bigg|_{(t_2)}$$

In Equation 10, the ratio b_i is constant at t_1 and t_2 , since the measurement point n stays the same. When a component is in a resonance condition at t_1 and t_2 , the mode shape of the same resonance stays the same. The ratio a_i and phase difference θ_i are also constant, provided the system is linear. The summation factor

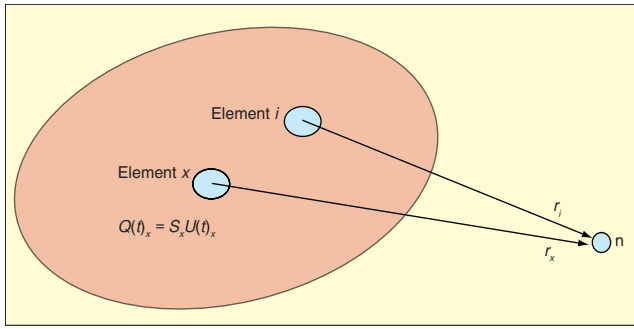


Figure 1. Elements x and i as point monopoles.

given by Equation 11 equals one.

$$SF = \frac{\sum_{i=1}^J \left(\frac{a_i}{b_i} e^{-j(kb_i r_x + \theta_i - kr_x)} \right)_{(t_1)}^2 \sum_{i=1}^J \left(\frac{a_i}{b_i} e^{-j(kb_i r_x + \theta_i - kr_x)} \right)_{(t_2)}}{\sum_{i=1}^J \left(\frac{a_i}{b_i} e^{-j(kb_i r_x + \theta_i - kr_x)} \right)_{(t_1)}^2 \sum_{i=1}^J \left(\frac{a_i}{b_i} e^{-j(kb_i r_x + \theta_i - kr_x)} \right)_{(t_2)}} = 1 \quad (11)$$

and

$$\frac{I_n(t_1)}{I_n(t_2)} = \frac{p_n(t_1)^2}{p_n(t_2)^2} \quad (12)$$

A study was conducted on engine covers.⁴ These covers were simulated by a 0.524 m × 0.236 m steel plate with various uniform thicknesses. The fundamental modes start at 30 and 110 Hz for the 1- and 3-mm-thick plates, respectively. The edge mode starts at 677 Hz. Above this frequency, the radiation efficiency increases significantly, from 20 dB (3-mm-thick plate) to 30 dB (1-mm-thick plate), as resonances reach coincidence frequency. Since radiated sound power is proportional to radiation efficiency, the plate response is primarily dominated by resonances from 800-2500 Hz throughout the entire speed range. Many resonances have repeatedly been excited at any t_1 and t_2 , and the engine noise is dominated by these resonances. The summation factor of Equation 11 will be close to one. Thus,

$$\frac{I_n(t_1)}{I_n(t_2)} \approx \frac{p_n(t_1)^2}{p_n(t_2)^2} \quad (13)$$

Therefore, one can estimate average sound intensity at low speed from the measurements and at high speeds by scaling. There is no restriction on Equation 7 for the location of point n , except that $p_n(t)$ cannot be zero. Sound pressure $p_n(t)$ fluctuates as the measurement point n moves toward the measurement surface in the acoustic near field.⁵ But it is also susceptible to contamination from adjacent components when the measurement point n moves away from the measurement surface. Based on our test results, if this point is selected correctly, adjacent components will not affect the sound intensity scaling calculation unless there is a dominant resonance, which is correctable.

Based on Equation 13, it can be shown that 1 pressure measurement point gives the same results as an average of multiple points as long as $p_n(t)$ does not equal zero. To avoid the slight possibility of zero mean square pressure amplitude, two measurement points are recommended for large surface components. The spatial variation of sound intensity is accommodated by baseline measurements.

Experimental Scaling Tests

Experimental tests to evaluate the sound intensity scaling method were conducted in a hemi-anechoic test cell. They include:

- Comprehensive set of sound intensity data (surface average) at a base speed (2000 rpm) at wide open throttle (WOT).
- Repeated sound intensity data for measurement system analysis at 1500 and 2000 rpm at WOT.
- Discrete-point SPL data from the speed range of interest, usually 1000 to 6000 rpm, at WOT.
- Repeated discrete-point SPL data for measurement system analysis from 1000 rpm to 6000 rpm at WOT.
- Discrete-point sound intensity data for verification of scaled

high-speed sound intensity estimates at 1500, 2000, 3000 and 4000 rpm at WOT.

- Additional SPL data for evaluation of adjacent component wrapping from 1500 to 6000 rpm at WOT.

Data at base speed are baselines for sound intensity scaling calculations. Point tests are used to verify sound intensity scaling calculation results. SPL tests are used to calculate SPL ratio for sound intensity scaling calculation.

The sound intensity scaling calculation is straightforward. First, extract component SPL data for each individual speed from the run-up measurements. Then calculate SPL differences between engine speed n and the base speed at each 1/3-octave band. Speed n could be any speed from 1000 to 6000 rpm except the base speed. Finally, sound intensity level can be scaled based on equation 13.

Verification Results

To verify the scaling method, measured and estimated sound intensity data were compared. Component surface average data at 2000 rpm at WOT were collected as a baseline for sound intensity scaling calculations and fixed point measurements at 1500, 2000, 3000 and 4000 rpm at WOT for verification. Three components were selected: right cam cover, trans barrel top, and crankshaft pulley. Multiple points were used to cover spatial variation in the fixed-point measurements. The data points for each component were averaged to provide a single value for each component at each engine speed. The fixed-point sound intensity data for 2000 rpm were compared for each of the three components to the sound intensity data (surface average by sweep) as a check on how well the batch of individual measurement locations matched the continuous sweep result. The fixed-point data at 3000 and 4000 rpm then provided six independent calculations with which to judge the accuracy of the scaling method.

These measurements were compared to corresponding estimates of sound intensity that were derived using Equation 15. The results for estimated and measured sound intensity are listed in Table 1. The overall range of these differences is virtually the same as the measured resolution of ±0.7 dB calculated for the sweep measurements. Therefore, the scaling method is reliable to within the repeatability and reproducibility that can be expected from the measured sound intensity.

Application

More than 10 power plants have been tested with this methodology. Power plant noise contribution analyses (PNCA) have been conducted for several programs during NVH target setting and roadmap development. As an example, more than 10 individual component NVH actions were evaluated per PNCA, and seven of them were selected that offered the best NVH value significantly improving power plant radiated noise. Test data showed that radiated noise refinements achieved one of the world's quietest power plants. In conjunction with vehicle interior noise contribution analysis (INCA2), individual NVH performance at the vehicle level can be analyzed as well. This tool is very effective for power plant NVH evaluation early in the design stage.

Conclusions

The ratio of sound intensities measured for a given power plant component at two different engine speeds is proportional to the corresponding ratio of sound pressures squared in a resonance condition. With theoretical justification and experimental verification, a scaling method is proposed that, by tracking SPL from engine run-up data, sound intensity can be estimated for any engine speed from measurements at other speeds. This capability

Table 1. Difference in measured and estimated sound intensity.

Component	Calculated - Measured	
	OA, dB @ 3000 rpm	OA, dB @ 3000 rpm
Right cam cover	± 0.63	± 0.63
Trans barrel top	± 0.49	± 0.43
Crankshaft pulley	± 0.33	± 0.31

is valuable, because the conventional sound intensity measurements are made with a hand-held probe, and personnel within a test cell are limited to a maximum engine speed of 2500 rpm by safety regulations.

The test data show that the difference between the measured and calculated sound intensity levels among three components, in six test cases, with various engine speeds are within ± 0.63 dB. This method is therefore acceptable for sound source ranking.

A single microphone per component is sufficient for the scaling method. In a test to compare a single microphone measurement with an average of several for the same component, it was found that 96% of the differences from a run-up broken down into 50 rpm intervals were within ± 0.6 dB.

Sound intensity scaling makes it possible for power-plant source ranking and noise contribution analysis. The technique provides a huge advantage in NVH target setting and roadmap development early in the power plant design stage.

Acknowledgement

Appreciation goes to Mark Stickler and Mark Clapper for their review of this article. We would also like to thank Bruce Tobis, Larry Obourn, Deb Paul, and Fred Stone for their support of testing, data processing and analysis.

References

1. Zeng, Paul, "Target Setting Procedures for Vehicle Powerplant Noise Reduction," *Sound & Vibration*, July 2003.
2. Fahy, F. J., *Sound Intensity*, E & FN Spon, an imprint of Chapman & Hall, London, 1995.
3. Reynolds, Douglas D., "Engineering Principles of Acoustics-Noise and Vibration Control," Las Vegas: D.D.R. Inc., 1985.
4. Institute of Sound & Vibration Research, "A Simple Analytical Model Describing the Physical Parameters Which Control the Sound Power Radiated by an Engine Cover When Idealized as a Flat Rectangular Plate of Uniform Thickness," ISVR Contract Report No. 99/32, September 1999.
5. Kinsler, Lawrence E., *Fundamentals of Acoustics*, John Wiley & Sons, New York, January 1980. 

The author can be reached at: pzeng@ford.com.